Analysis of ground states of 0-π long Josephson junctions

A. Zenchuk*

Center of Nonlinear Studies of L. D. Landau Institute for Theoretical Physics (International Institute of Nonlinear Science), Kosygina 2, Moscow 119334, Russia

E. Goldobin†

Institut für Mikro- und Nanoelektronische Systeme, Universitat Karlsruhe (TH), Hertzstrasse 16, D-76187 Karlsruhe, Germany and Physikalisches Institut-Experimentalphysik II, Universität Tübingen, Auf der Morgenstelle 14, D-72076 Tübingen, Germany

(Received 26 April 2003; revised manuscript received 18 August 2003; published 23 January 2004)

We investigate analytically a long Josephson 0-π junction with several 0 and π facets which are comparable to the Josephson penetration length λ_J. Such junctions can be fabricated exploiting (a) the *d*-wave order-parameter symmetry of cuprate superconductors; (b) the spacial oscillations of the order parameter in superconductor-insulator-ferromagnet-superconductor structures with different thicknesses of ferromagnetic layer to produce 0 or π coupling; or (c) the structure of the corresponding sine-Gordon equations and substituting the phase π discontinuities by the artificial current injectors. We investigate analytically the possible ground states in such a system and show that there is a critical facet length a_c, which separates the states with half-integer flux quanta (semifluxons) from the trivial ''flat phase state'' without magnetic flux. We analyze different branches of the bifurcation diagram, derive a system of transcendental equations which can be effectively solved to find the crossover distance a_c (bifurcation point), and present the solutions for different number of facets and the edge facets length.

DOI: 10.1103/PhysRevB.69.024515 PACS number(s): 74.50.+r, 85.25.Cp, 74.20.Rp

I. INTRODUCTION

Due to the recent progress in technology it is now possible to fabricate different types of π Josephson junctions (JJ): high-T_c tricrystal grain-boundary JJ,[1] $YBa_2Cu_3O_7$-Nb zigzag ramp JJ,[2] superconductor-ferromagnet-superconductor (SFS),[3,4] or superconductor-insulator-ferromagnet-superconductor (SIFS).[5] π junctions are very promising elements for Josephson electronics. It was already suggested that they can be used in analog[6] and digital[7,8] circuits in classical regime and for implementation of qubits.[9]

In this paper, we focus on *long* Josephson junctions (LJJ) consisting of several 0 and π parts (facets). We will call such junctions 0-π-LJJ's. LJJ consisting of very short (and random) 0 and π facets, which are naturally formed in 45° high-T_c grain boundaries, were studied by Mints and coauthors in a series of works (see Ref. 10 and references therein). We are more interested in facets with the length a comparable to the Josephson penetration depth λ_J such as in artificially prepared structures. These are the sizes which will be used in potential devices based on fractional vortex dynamics, both in classical and in quantum ones.[11,12]

It was found[13,14] that at the point where 0 and π facets join, a new type of nonlinear excitation may appear. This new nonlinear solution of the properly modified sine-Gordon equation looks like a vortex and contains one-half of the flux quantum and therefore is called ''semifluxon.'' The semifluxon (SF) is always pinned at the joining point between 0 and π facets. The presence of SF was demonstrated experimentally[15] by scanning super conducting quantum interference device microscopy on $YBa_2Cu_3O_7$-Nb ramp zigzag LJJ in the *long facet limit*, i.e., when the length of the facets $a \gg \lambda_J$. SF's were also experimentally observed in the tricrystal grain-boundary LJJ's.[16–18]

In this work we study analytically the ground states of 0-π-LJJ with arbitrary number of alternating 0 and π facets and the effect of edge facets on the type of the ground state. As it was shown earlier for some particular cases, there is a critical facet length a_c which separates the domains with the two most natural lowest-energy configurations: the flat phase state and antiferromagnetically (AFM) ordered array of semifluxons.

The joining points between 0 and π facets we will call a phase discontinuity points since, e.g., in $YBa_2Cu_3O_7$-Nb zigzag LJJ, the Josephson phase $\phi(x)$ is π discontinuous at these points. In the other types of junctions, e.g., SFS and SIFS, the Josephson phase is continuous, but one can finally arrive to the same equations making a proper substitution of variables: $\phi(x,t)=\mu(x,t)+\theta(x)$.[14] Following Ref. 14 and regardless of the LJJ type we will denote discontinuous phase as $\phi(x)$, while continuous (magnetic) component of the phase as $\mu(x)$.

In Sec. II we introduce the model and represent general solution $\mu(x)$ for arbitrary distribution of π-discontinuity points and present several examples. In Sec. III, we calculate the crossover distances a_c (corresponding to ''AFM ordered SF chain''—''flat phase state'' transition) for N equidistantly distributed π-discontinuity points with the arbitrary length b of edge facets. Finally Sec. IV summarizes our results.

II. MODEL AND GENERAL STATIONARY SOLUTION

We consider finite length Josephson junction with N ''0-π'' conjunction points (π-discontinuity points). Let the coordinates of these points be x_j, $j=1,\dots,N$, and the coordinates of the two ends of LJJ be x_0 and x_{N+1}, see Fig. 1. We will write and solve all equations in terms of the magnetic component of the phase $\mu(x)$ which is a continuous

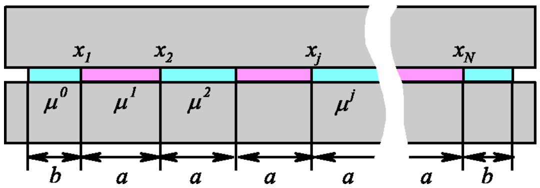

FIG. 1. Sketch of the 0-π-LJJ with notations used.

function.[14] Let $\mu^j(x)$, $j=0,\dots,N$, be the piece of $\mu(x)$, inside jth interval $x_j \leqslant x \leqslant x_{j+1}$. Thus in total we have $N+1$ intervals enumerated by $j=0,1,\dots,N$. μ^{2n}, $n=0,1,\dots$ correspond to "0" intervals, and μ^{2n+1}, $n=0,1,\dots$ correspond to "π" intervals. While we use superscript j to denote a piece of the function $\mu(x)$ at jth interval, we use the subscript j to denote the value of the function $\mu(x)$ at $x=x_j$, i.e., $\mu_j=\mu(x_j)$, $j=0,\dots,N+1$. Since we will look for a continuous solution $\mu(x)$, μ_j are uniquely defined.

In these notations the sine-Gordon equation reads[14]

$$\mu^j_{xx}-\mu^j_{tt}=(-1)^j \sin \mu^j. \tag{1}$$

Later on, we will need the above time-dependent equation for analysis of stability of some solutions. At this moment we write only the stationary version of Eq. (1) which has the form

$$\mu^j_{xx}=(-1)^j \sin \mu^j. \tag{2}$$

It may be integrated once

$$(\mu^j_x)^2=C_j-2(-1)^j \cos \mu^j, \quad j=0,1,\dots,N, \tag{3}$$

where C_j are integration constants for jth interval. We look for solutions with arbitrary, but equal boundary conditions $\mu_x(x_0)=\mu_x(x_{N+1})=h$, which correspond to the uniform applied magnetic field h.

End points x_0 and x_{N+1} may be either finite or infinite. Infinitely long JJ is considered as limit of finite JJ. First we construct solutions for finite length LJJ.

A. General stationary solution for finite length JJ

We require that the derivative μ_x is continuous at $x=x_j$, i.e., $\mu^j_x(x_j)=\mu^{j+1}_x(x_j)$, $j=1,\dots,N$. Then

$$C_0=\mu^0_x(x_0)^2+2\cos\mu_0,$$

$$\begin{aligned} C_j&=C_{j-1}+4(-1)^j\cos\mu_j\\ &=\mu^0_x(x_0)^2+2\cos\mu_0+4\sum_{i=1}^{j}(-1)^i\cos\mu_i,\\ &\quad j=1,\dots,N,\\ C_N&=\mu^N_x(x_{N+1})^2+2(-1)^N\cos\mu_{N+1}. \end{aligned} \tag{4}$$

The above system involves two different expressions for C_N, which produce the first relation among μ_j:

$$2\cos\mu_0+4\sum_{i=1}^{N}(-1)^i\cos\mu_i=2(-1)^N\cos\mu_{N+1}. \tag{5}$$

After the integration of Eq. (3) one gets inside the jth interval:

$$\begin{aligned} x-x^*_j&=\pm\int_{2\pi n_j+\sigma_j\pi}^{\mu}\frac{d\nu}{\sqrt{C_j+2\cos(\nu+\sigma_j\pi)}}\\ &=\alpha_j\int_0^{(\mu-\sigma_j\pi-2\pi n_j)/2}\frac{d\nu}{\sqrt{1-\alpha_j^2\sin^2\nu}}\\ &=\alpha_j F[(\mu^j-\sigma_j\pi-2\pi n_j)/2,\alpha_j^2], \end{aligned} \tag{6}$$

$$\alpha_j=\pm\frac{2}{\sqrt{C_j+2}}, \tag{7}$$

where n_j are some integers which may be different for each particular interval; $F(x,m)$ is the elliptic integral of the first kind; the lower limit of integration in the first integral is convenient for representation of the final result in terms of elliptic functions. To write such limits of integration we use x^*_n ($\neq x_n$) in the above equations. The integration constants x^*_j can be expressed in terms of μ_j ($j=0,\dots,N$):

$$x^*_j=x_j-\alpha_j F[(\mu_j-\sigma_j\pi-2\pi n_j)/2,\alpha_j^2], \tag{8}$$

where the sign of α_j is taken from the condition that x increases when one goes along the junction. It is altering in each extremum of the function $\mu(x)$; the variable σ is such that $\sigma_{2n}=1$, $\sigma_{2n+1}=0$, $n=0,1,\dots,N$. Functions $\mu^j(x)$ can be expressed in terms of elliptic functions from Eq. (6):

$$\mu^j=2\pi n_j+\sigma_j\pi+2\,\mathrm{am}\left[\frac{x-x^*_j}{\alpha_j},\alpha_j^2\right], \tag{9}$$

where $\mathrm{am}(x,m)$ is the Jacobi amplitude. The values μ_j, $j=0,\dots,N+1$, are the solutions of the following system of $N+1$ equations ($j=0,\dots,N$):

$$\mu_{j+1}=2\pi n_j+\sigma_j\pi+2\,\mathrm{am}\left[\frac{x_{j+1}-x^*_j}{\alpha_j},\alpha_j^2\right], \tag{10}$$

and Eq. (5).

Below we will need extremum values of μ^j (if any),

$$\mu^j_{\mathrm{ex}}=\pm\arccos\left(\frac{(-1)^j C_j}{2}\right)+2\pi n_j. \tag{11}$$

Remember that the behavior of the function $\mu^j(x)$ is defined by the value of the constant C_j, namely,

$$|C_j|<2:\quad \mu^j(x)\ \text{ is nonmonotonic function,} \tag{12}$$

$$|C_j|\geqslant 2:\quad \mu^j(x)\ \text{ is monotonic function.} \tag{13}$$

From the above one can get the following restriction on the possible values of the parameters n_j: if $\mu^j_x(x_j)>0$, then $n_{j+1}\geqslant n_j$; if $\mu^j_x(x_j)<0$, then $n_{j+1}\leqslant n_j$.

Thus Eq. (9) together with Eqs. (8) and (10) represents general formulas for all possible ground states in 0-π-LJJ of finite length with arbitrary number of discontinuity points and uniform magnetic field. Each particular ground states is characterized by the parameters n_j and μ_j. The later are solutions of the system (10). We emphasize that this system may be either solvable or not, which depends on values n_j and positions of discontinuity points x_j.

B. General stationary solution for infinitely long JJ

In this section we give some remarks regarding stationary solutions for infinitely long JJ. The main difference between finite and infinite length is related to the edge facets. Let us consider the limit $x_0 \rightarrow -\infty$, $x_{N+1} \rightarrow \infty$, i.e., the number of facets is still finite and equal to N, but the edge facets are infinitely long.

The boundary conditions assume that magnetic field μ_x disappears at $x \rightarrow \pm\infty$. Since the first and the last facets have infinite length, the value of the phase at $\pm\infty$ should be such that the system has zero energy per unit of the facet length. Otherwise the total energy of the system is infinite.[19] To have finite energy the phase should be equal to $2\pi k$ (if the edge facet is a 0 facet) or to $k(2\pi+1)$ (if the edge facet is a π facet). Thus, we admit the following boundary conditions:

$$\lim_{x \rightarrow \pm\infty} \mu_x = 0, \tag{14a}$$

$$\lim_{x \rightarrow -\infty} \mu = 0, \tag{14b}$$

$$\lim_{x \rightarrow +\infty} \mu = 2\pi n_N + (1-\sigma_N)\pi. \tag{14c}$$

Equations (4) now have the form

$$C_0 = C_N = 2,$$

$$C_j = C_{j-1} + 4(-1)^j \cos\mu_{j-1} = 2 + 4\sum_{i=1}^{j} (-1)^i \cos\mu_i, \quad j = 1, \ldots, N. \tag{15}$$

Equation (5) is reduced to the following one:

$$\sum_{i=1}^{N} (-1)^i \cos\mu_i = 0. \tag{16}$$

Expression (11) for μ_{ex}^j as well as Eqs. (8)–(10) stay the same for the inner intervals. But for the edge facets ($j = 0, N$), Eqs. (9), should be replaced with

$$\mu^0(x) = 4 \arctan[G_0 \exp(x\, s_1)], \tag{17a}$$

$$\mu^N(x) = (1-\sigma_N)\pi + 4 \arctan[G_N \exp(x s_N)] + 2\pi n_N, \tag{17b}$$

where parameters s_1 and s_N may be either 1 or (-1) depending on boundary conditions at infinities (14). They define whether the function is increasing or decreasing. Integration constants G_0 and G_N are defined by the equations

$$\mu^0(x_1) = 4 \arctan[G_0 \exp(x_1 s_1)], \tag{18a}$$

$$\mu^N(x_N) = (1-\sigma_N)\pi + 4 \arctan[G_N \exp(x_N s_N)] + 2\pi n_N. \tag{18b}$$

C. Examples of particular solutions

The problem to construct solutions is reduced to solving the system (5) and (10). We consider examples of two types of solutions: the so-called AFM state $\uparrow\downarrow\uparrow\downarrow$ and the state $\uparrow\uparrow\downarrow\downarrow$ for LJJ with equidistant distribution of discontinuity points x_j,[19] zero-field boundary conditions

$$\mu_x(x_0) = \mu_x(x_{N+1}) = 0 \tag{19}$$

and $n_j = 0$ for all j. Thus $0 < \mu < 2\pi$,

$$\mu_{\mathrm{ex}}^j = \arccos\left(\frac{(-1)^j C_j}{2}\right). \tag{20}$$

In this case expression for α_j in Eqs. (6)–(13) can be given in the following form:

$$\alpha_j = \frac{2 \,\mathrm{sgn}\, \mu_x(x_j)}{\sqrt{C_j+2}}, \quad j = 1, \ldots, N, \quad \alpha_0 = -\frac{2}{\sqrt{C_0+2}}. \tag{21}$$

Following Ref. 19, we consider equidistant distribution of discontinuity points $x_j = a(j-1)$, $j = 1, \ldots, N$, but with end points $x_0 = -b$ and $x_{N+1} = a(N-1)+b$, where b is the length of the edge facets which may be different from a, as shown in Fig. 1. Due to the symmetry one has

$$\text{For even } N, \quad j = 0, \ldots, N/2: \quad \mu_j = \mu_{N+1-j}, \tag{22a}$$

$$\text{For odd } N, \quad j = 0, \ldots, (N-1)/2: \quad \mu_j = \pi - \mu_{N+1-j}, \quad \mu_{(N+1)/2} = \pi/2. \tag{22b}$$

a. AFM state in finite length LJJ. For AFM state, μ^j should have extremum value inside its interval, which, according to Eq. (12), means that $C_j < 2$ for all j. The plots of $\phi(x)$, $\mu(x)$, $\mu_x(x)$ for $a = 2$, $b = 5$ and two different values of N ($N = 3$ and $N = 4$) are shown in Fig. 2.

b. $\uparrow\uparrow\downarrow\downarrow$ state in infinite LJJ. Let us consider infinitely long JJ with $N = 4$. For this state μ^j should have extremum value inside the middle interval: $C_1, C_3 > 2$; $C_0 = C_4 = 2$, and $0 < C_2 < 2$. Parameters in Eqs. (17) and (18) are defined as follows: $\sigma_N = 1$, $s_1 = 1$, $s_2 = -1$. The plots of $\phi(x)$, $\mu(x)$, $\mu_x(x)$ are shown in Fig. 3

III. CROSSOVER DISTANCE

In this section we study the transition between flat phase state and AFM ordered SF state in 0-π-LJJ with equidistant distribution of π-discontinuity points $|x_{j+1} - x_j| = a$, $j = 1, \ldots, N-1$ expressing the length of the edge facets in terms of a: $b = \beta a$. For this case $0 \leqslant \mu \leqslant \pi$.

In Sec. III A we study the stability of the flat phase solution and derive the system of algebraic equations for calculation of a_c. In Sec. III B we study the existence of AFM

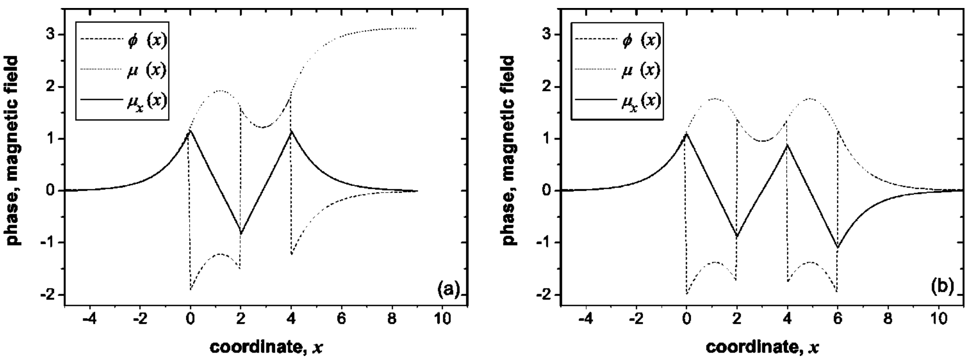

FIG. 2. The state with AFM ordered SF's. Graphs of $\phi(x)$, $\mu(x)$, and $\mu_x(x)$ for $a=2$, $b=5$; (a) $N=3$, $\mu_0=0.0172$, $\mu_1=1.2371$ and (b) $N=4$, $\mu_0=0.016$, $\mu_1=1.1569$, $\mu_2=1.3775$.

solution and derive another system of equations defining a_c.

A. Stability of flat phase state

We study solutions of the time-dependent equation (1) which have small amplitude oscillations around the flat state μ_c. As it follows from Eq. (2), the value of phase $\mu(x)=\mu_c$ in the flat phase state can be either 0 or π. Note that for odd N the symmetry conditions (22b) result in $\mu=\pi/2$ at the middle point $x=x_{N/2}$. Since $\mu(x)=\text{const}$ in the flat phase state, μ should be equal to $\pi/2$, but this is not a solution of Eq. (1). Thus, we conclude that for odd N the flat phase state cannot be realized, so we formally take $a_c=0$. Below we consider only even N.

Let us introduce a new function $\tilde{\mu}=\mu-\mu_c \ll 1$ for which Eq. (1) has one of the forms given below

$$\tilde{\mu}^j_{xx}-\tilde{\mu}^j_{tt}=(-1)^j\tilde{\mu}, \quad \mu_c=0, \tag{23a}$$

$$\tilde{\mu}^j_{xx}-\tilde{\mu}^j_{tt}=(-1)^{j+1}\tilde{\mu}, \quad \mu_c=\pi \tag{23b}$$

for all $j=0,\ldots,N+1$.

First, we study only Eq. (23a) corresponding to $\mu_c=0$. To study the stability we look for the solution in the following form:

$$\tilde{\mu}^j=e^{\sqrt{E}t}\nu^j, \tag{24}$$

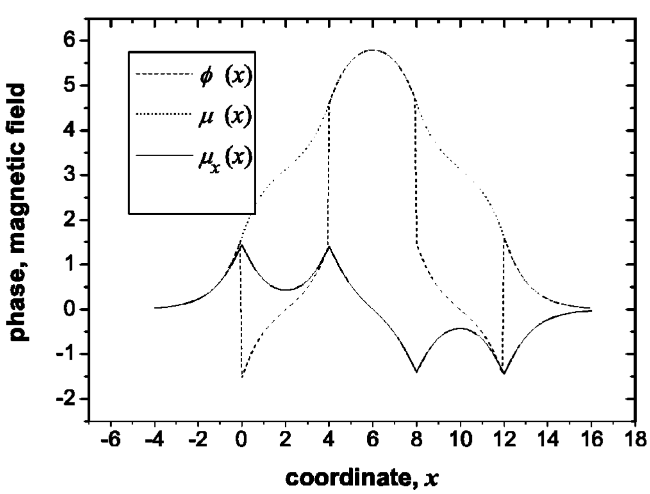

FIG. 3. The state $\uparrow\uparrow\downarrow\downarrow$. Graphs of $\phi(x)$, $\mu(x)$, and $\mu_x(x)$ for infinitely long JJ with $a=4$ and $N=4$; $\mu_1=1.6165$, $\mu_2=4.6086$.

where E is considered around $E=0$, because this is the point where the stability of solution changes. Hereafter we use $-1<E<1$. Then Eq. (23a) gets the form

$$\nu^j_{xx}=[E+(-1)^j]\nu^j, \quad j=0,\ldots,N+1. \tag{25}$$

There are two solutions of the correspondent characteristic equation: $k=\pm k_1$ for even intervals and $k=\pm ik_2$ for odd intervals, where $k_1=\sqrt{1+E}$ and $k_2=\sqrt{1-E}$ are both real. The solutions of Eqs. (25) can be represented by the following system:

$$\nu^0=A_0\cosh(k_1x+\beta_0), \tag{26a}$$

$$\nu^j=A_j\cosh[k_1\{x-a(j-1)\}+\beta_j], \quad j=2,4,\ldots, \tag{26b}$$

$$\nu^j=A_j\cos[k_2\{x-a(j-1)\}+\beta_j], \quad j=1,3,\ldots. \tag{26c}$$

The zero-field boundary condition $\mu_x(-\beta a)=0$ gives the formula for β_0: $\beta_0=\beta a$. Due to the symmetry (22b), it is enough to consider only half of the whole LJJ. We have for the middle interval $\mu_{N/2}=\mu_{N/2+1}$, which gives expressions for $\beta_{N/2}$: $\beta_{N/2}=-k_1a/2$ for even $N/2$ or $\beta_{N/2}=-k_2a/2$ for odd $N/2$. Continuity of the functions μ imposes the following relations among parameters A_j and β_j:

$$A_0\cosh(\beta a)=A_1\cos(\beta_1), \tag{27a}$$

$$A_j\cos(k_2a+\beta_j)=A_{j+1}\cosh(\beta_{j+1}), \quad j=1,3,\ldots, \tag{27b}$$

$$A_j\cosh(k_1a+\beta_j)=A_{j+1}\cos(\beta_{j+1}), \quad j=2,4,\ldots. \tag{27c}$$

To provide continuity of μ_x, one needs to impose additional relations among the parameters β_j:

$$k_1\tanh(\beta a)=-k_2\tan(\beta_1), \tag{28a}$$

$$k_2\tan(k_2a+\beta_j)=-k_1\tanh(\beta_{j+1}), \quad j=1,3,\ldots, \tag{28b}$$

$$k_1\tanh(k_1a+\beta_j)=-k_2\tan(\beta_{j+1}), \quad j=2,4,\ldots, \tag{28c}$$

where $j<N/2$. Equations (27) define the amplitudes A_j, $j>0$, in terms of A_0 and β_n, $n=0,\ldots,N/2$. Equation (28a) establishes relation between a and E, while Eqs. (28b) and (28c) define parameters β_j.

The solution (24) is stable if $E\leqslant 0$. We define crossover distance a_c the distance for which $E=0$ and, consequently, $k_1=k_2=1$, i.e., the system of Eqs. (28a)–(28c) defining a_c is

$$\tanh(\beta a_c)=-\tan(\beta_1), \tag{29a}$$

$$\tan(a_c+\beta_j)=-\tanh(\beta_{j+1}), \quad j=1,3,\ldots, \tag{29b}$$

$$\tanh(a_c+\beta_j)=-\tan(\beta_{j+1}), \quad j=2,4,\ldots, \tag{29c}$$

$$\beta_{N/2}=-\frac{a_c}{2}. \tag{29d}$$

Note that this system of equations is rather easy to solve consequently excluding β_j. At the end one gets a transcendental equation (29a) for a_c, with given parameter β and function $\beta_1(a_c)$. It is clear that $a_c=0$ and all $\beta_j=0$ is solution of the system (29). Instead, we are interested to find the first nonzero solution a_c of Eq. (29).

Nonzero solution to this transcendental equation does not exists for any β. To derive the existence conditions we analyze the behavior of the function $\beta_1(a)$ in Appendix B, where it is proven that $\beta_1(a_c)$ is a decreasing and convex function within the interval from $a_c=0$ to the first discontinuity. Thus, $\tan[-\beta_1(a_c)]$ is increasing and concave, so that Eqs. (29) have nontrivial solution only if

$$\tanh'(\beta a_c)|_{a_c\to 0}>\tan'[-\beta_1(a_c)]|_{a_c\to 0},$$

i.e., if $\beta>1/2$. Using Eq. (28a) we have

$$\sqrt{\frac{E+1}{1-E}}=\frac{\tan[-\beta_1(a)]}{\tanh(\beta a)}\leqslant 1 \tag{30}$$

and, consequently, $E\leqslant 0$ inside the interval $0\leqslant a\leqslant a_c$.

We have found that for any $\beta>1/2$ there is an interval $0<a<a_c$ where the flat phase state $\mu_c=0$ is stable. If $\beta<1/2$, then $E>0$ and the flat phase state $\mu_c=0$ is unstable. Thus, $\beta=1/2$ is a threshold value, for which $E=0$ and Eq. (29) has only trivial solution.

In a similar way, one can show that the flat phase state $\mu_c=\pi$, corresponding to Eq. (23b), is stable inside the interval $0<a<a_c$, if $\beta<1/2$. The appropriate system defining a_c is

$$\tan(\beta a_c)=-\tanh(\beta_1), \tag{31a}$$

$$\tanh(a_c+\beta_j)=-\tan(\beta_{j+1}), \quad j=1,3,\ldots, \tag{31b}$$

$$\tan(a_c+\beta_j)=-\tanh(\beta_{j+1}), \quad j=2,4,\ldots, \tag{31c}$$

$$\beta_{N/2}=-\frac{a_c}{2}. \tag{31d}$$

TABLE I. The values of $a_c^{(N)}$ for $\beta=1/4,1,2,\infty$ corresponding to instability of flat phase state (accuracy of calculation is ± 0.0001).

	a_c			
N	$\beta=1/4$	$\beta=1$	$\beta=2$	$\beta=\infty$
2	2.92771	1.4639	1.5670	$\pi/2$
4	1.25461	1.1772	1.2989	1.3063
6	0.98327	1.0060	1.1245	1.1343
8	0.83438	0.8914	1.0032	1.0146
10	0.73731	0.8082	0.9134	0.9259

The consideration of this system is similar to that given for Eq. (29) in Appendix B. Again the solvability of the whole system (31) depends on the existence of the nontrivial solution of Eq. (31a). Now the functions $\beta_j(a_c)$ with even j are decreasing and convex. Expression for β_1 comes from Eq. (31b),

$$\beta_1(a_c)=-a_c-\operatorname{arctanh}\tan\beta_2(a_c).$$

This function is concave, which is enough to arrive to the conclusion that the first equation of Eq. (31) has nonzero solution in the subdomain from $a_c=0$ to the first discontinuity provided $\beta<1/2$.

The values of a_c corresponding to the instability of the flat phase state are calculated using Eqs. (29) and (31) for $\beta=\frac{1}{4},1,2,\infty$, and summarized in Table I. One can check that the values in this table are in accordance with those obtained earlier by direct numerical simulation[19] for $\beta=1/2,1$. The result for $N=2$ and $\beta=\infty$ coincides with the one calculated earlier analytically.[11,20] We stress here that our present results are obtained for arbitrary edge facet length b (arbitrary β) and have much higher accuracy (can be calculated much faster).

The plot $a_c^{(N)}(\beta)$ for different N can be seen in Fig. 4. As $\beta\to 0$, $a_c^{(2)}\to\infty$ while for $N>2$ $a_c^{(N)}$ approaches some finite value. Also note the following natural property which can be seen in Fig. 4: $a_c^{(N)}(1)=a_c^{(N+2)}(0)$. The fact that $a_c^{(2)}\to\infty$ for $\beta\to 0$ means that 0-π-0 LJJ approaches the limit of all-π LJJ, where vortex solutions are unstable and flat phase state wins.

1. Behavior of instability point at large N

Using the systems (29) and (31) its possible to determine a ground state of a very large LJJ, i.e., when $N\to\infty$.

First, let us consider the case $\beta<1/2$. As we saw above, according to the system (31) when $a_c\to 0$, the values of $\beta_j\sim a_c$. We write $\beta_j=a_c\psi_j$, where $\psi_j\sim 1$. In this case we expand the equations of the system (31) in Taylor series for small a_c and discard all the terms smaller than $O(a_c^3)$:

$$\beta\approx-\psi_1+\frac{2}{3}a_c^2\psi_1^3,$$

$$\psi_j\approx-1-\psi_{j+1}-\frac{2}{3}a_c^2\psi_{j+1}^3, \quad j=1,3,\ldots,$$

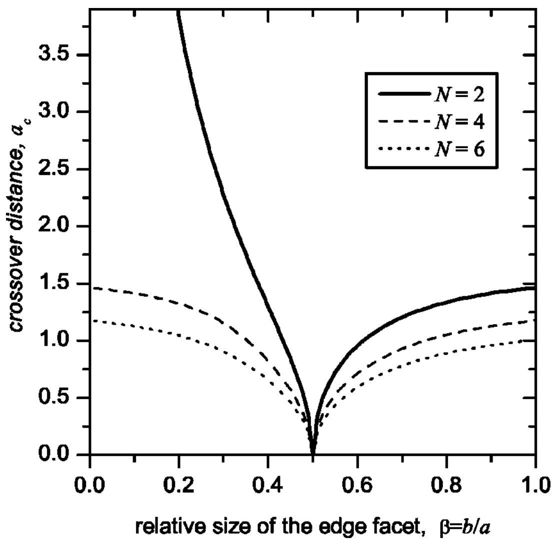

FIG. 4. The dependences of crossover distances $a_c^{(2)}$, $a_c^{(4)}$, and $a_c^{(6)}$ on β. These curves can be obtained by solving either stability problem [Eqs. (29) for $b>a/2$ or Eqs. (31) for $b<a/2$] or AFM solution existence problem [Eqs. (46) for $b>a/2$ and Eqs. (47) for $b<a/2$].

$$\psi_j \approx -1-\psi_{j+1}+\frac{2}{3}a_c^2\psi_{j+1}^3, \quad j=2,4,\ldots,$$

$$\psi_{N/2}=-1/2. \tag{32}$$

Substituting expressions for ψ_j one by one starting with the last equation and discarding all the terms smaller than $O(a_c^2)$ we result in the final expressions for ψ_j,

$$\psi_j=-\frac{1}{2}+(-1)^{j+1}\left(\frac{N}{2}-j\right)\frac{a_c^2}{12}. \tag{33}$$

Thus, the first equation of the system (32) now reads

$$\beta\approx\frac{1}{2}-\frac{a_c^2}{24}N. \tag{34}$$

Finally, the expression for a_c is

$$a_c\approx\sqrt{\left(\frac{1}{2}-\beta\right)\frac{24}{N}}. \tag{35}$$

It is valid for $N \gg 24(1/2-\beta)$.

Second, for *finite* $\beta>1/2$ the reasoning is similar, and we get

$$a_c\approx\sqrt{\left(\beta-\frac{1}{2}\right)\frac{24}{N}}. \tag{36}$$

This approximation is valid for $N\gg 24(\beta-1/2)\max(1,\beta^2)$.

In the case $\beta\to\infty$ (*infinitely long edge facets*), $\tanh(\beta a_c)\to 1$ and our approximation does not work. The reason is that β_j does not vanishes with increase of N in this case. Alternative, more complex but also more exact, derivation of asymptotic behavior of a_c for $N\to\infty$ and any finite as well as infinite β is presented in Appendix C.

B. Existence of AFM ordered solution

In this section we apply the general formulas derived in Sec. II to calculate the crossover distance for AFM state in the LJJ with equidistant distribution of π-discontinuity points.

If one chooses a domain of parameters where AFM ordered SF chain is present, vary a and plot the solutions $\mu(x)$, he may notice that the amplitude of spatial oscillations of $\mu(x)$ decreases as a decreases, see Fig. 5. It may happen, as we show below, that the amplitude of $\mu(x)$ vanishes at some $a=a_c$ which may be larger than zero.

In this section we reintroduce the crossover distance a_c as a distance at which the amplitude of oscillations of $\mu(x)$ vanishes, i.e., $\mu(x)\to\mu_c$ for $a\to a_c+0$. In fact the limiting value of the phase μ_c can have only three different values: 0, $\pi/2$, π. To prove this, we refer to Eq. (6) and write the set of expressions for the distance $a=|x(\mu_j+1)-x(\mu_j)|$ $(j=1,\ldots,N-1)$ between discontinuity points

$$a=(-1)^{j+1}\left(\int_{\mu_j}^{\mu_{\rm ex}^j}\frac{d\nu}{\sqrt{C_j-2(-1)^j\cos\nu}}-\int_{\mu_{\rm ex}^j}^{\mu_{j+1}}\frac{d\nu}{\sqrt{C_j-2(-1)^j\cos\nu}}\right), \tag{37}$$

$j=1,\ldots,N$. For the left edge interval it reads

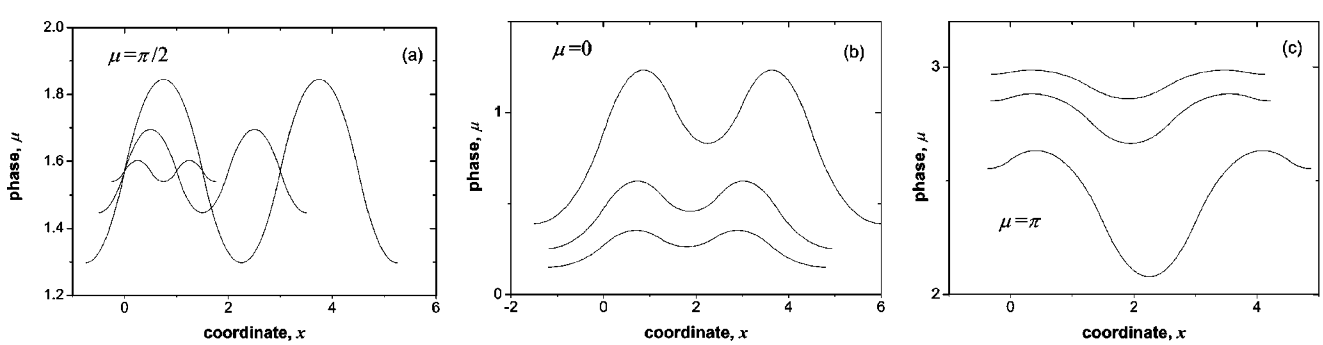

FIG. 5. Graphs of $\mu(x)$, amplitude decreases with decrease of a: (a) $b=a/2, N=4$; $a=3/2,1,1/2$, $\mu_c=\pi/2$; (b) $b=a, N=4$; $a=3/2,1.25,1.2$, $\mu_c=0$; (c) $b=a/4, N=4$; $a=3/2,1.3,1.27$, $\mu_c=\pi$.

$$\beta a = \int_{\mu^0}^{\mu_1} \frac{d\nu}{\sqrt{C_0 - 2\cos\nu}}. \tag{38}$$

Due to the symmetry conditions (22) we consider here only the left half of the junction. Note that in spite of index *j*, both sides of the expression (37) do not depend on the facet number *j*, since we consider equidistantly distributed discontinuity points. Consider the limit $a \to a_c + 0$, which means

$$\mu_j \approx \mu_c + \epsilon \tilde{\mu}_j, \tag{39}$$

where $\epsilon \to 0$. The integration intervals are proportional to ϵ. The denominator can be approximated using $\nu = \mu_c + \epsilon\tilde{\nu}$ as

$$\sqrt{-2\epsilon K_s \sin\mu_c - \epsilon^2 K_c \cos\mu_c},$$

where K_s and K_c do not depend neither on μ_c nor on ϵ. If $\mu_c = 0$ or $\mu_c = \pi$, the denominator in Eq. (37) is $\propto \epsilon$, which results in $a_c > 0$. Otherwise the denominator is $\propto \sqrt{\epsilon}$, so that $a_c = 0$.

For all other values of $\mu_c \neq 0$ and $\mu_c \neq \pi$, the denominator in Eq. (37) is constant and integral vanishes, i.e., $a_c = 0$. It is interesting that "all other values of μ_c" essentially mean $\mu_c = \pi/2$, see Appendix A for details. This also allows us to make a quick conclusion that $a_c = 0$ for odd *N*. Indeed, for odd *N*, due to the symmetry conditions (22b) $\mu_{(N+1)/2} = \pi/2$ for any *a*. Therefore, $\mu(x) \to \mu_c = \pi/2$ when *a* decreases. This automatically means that $a_c = 0$.

Summarizing our findings, one can get the following possible values of μ_c depending on a_c and β.

(1) $\mu_c = \pi/2$ for odd *N*, Fig. 5(a); in this case $a_c = 0$.

(2) $\mu_c = 0$ for even *N* and $\beta > 1/2$, Fig. 5(b); in this case $a_c > 0$.

(3) $\mu_c = \pi$ for even *N* and $\beta < 1/2$, Fig. 5(c); in this case $a_c > 0$.

Since, for odd *N* $a_c = 0$ is already known, we calculate a_c only for the last two cases.

Since for AFM state one has the symmetry (22a), it is enough to consider $j = 0, \ldots, N/2$ with condition $\mu(a_{N/2}) = \mu(a_{N/2-1})$.

Even N, $\beta > 1/2$, $\mu_c = 0$. Using Eq. (39) with $\mu_c = 0$ Eqs. (4) and (20) can be approximated as follows:

$$C_j \approx 2(-1)^j + \epsilon^2 \Sigma_j, \tag{40}$$

$$\mu_{\rm ex}^j \approx \epsilon\sqrt{(-1)^{j+1}\Sigma_j} = \epsilon\tilde{\mu}_{\rm ex}^j, \tag{41}$$

where we defined Σ_j as

$$\Sigma_j = -2\sum_{i=1}^{j} (-1)^i \tilde{\mu}_i^2 - \tilde{\mu}_0^2. \tag{42}$$

It follows from Eqs. (12) and (40) that $\Sigma_j > 0$ for odd *j* and $\Sigma_j < 0$ for even *j*.

In the limit $\epsilon \to 0$ Eqs. (37) and (38) become

$$a_c^{(N)} = (-1)^{j+1}\left(\int_{\tilde{\mu}_j}^{\tilde{\mu}_{\rm ex}^j} \frac{d\tilde{\nu}}{\sqrt{\Sigma_j + (-1)^j \tilde{\nu}^2}} - \int_{\tilde{\mu}_{\rm ex}^j}^{\tilde{\mu}_{j+1}} \frac{d\tilde{\nu}}{\sqrt{\Sigma_j + (-1)^j \tilde{\nu}^2}} \right), \quad j = 1, \ldots, N/2. \tag{43}$$

$$\beta a_c^{(N)} = \int_{\tilde{\mu}_0}^{\tilde{\mu}_1} \frac{d\tilde{\nu}}{\sqrt{\tilde{\nu}^2 - \tilde{\mu}_0^2}}. \tag{44}$$

For the sake of simplicity we introduce new variables $\xi_j = \tilde{\mu}_j/\tilde{\mu}_1$, $\xi_1 = 1$, and

$$\tilde{\Sigma}_j = \frac{\sqrt{(-1)^{j+1}\Sigma_j}}{\tilde{\mu}_1} = \sqrt{2(-1)^{j+1}\left(-\sum_{i=2}^{j} (-1)^i \xi_i^2 + 1 - \frac{\xi_0^2}{2} \right)}. \tag{45}$$

The integration of Eq. (43) separately for odd $j < N/2$, even $j < N/2$ and the integration of Eq. (44) give the system of equations for $a_c^{(N)}$ and miscellaneous variables ξ_j:

$$a_c^{(N)} = \pi - \arcsin\frac{\xi_{j+1}}{\tilde{\Sigma}_j} - \arcsin\frac{\xi_j}{\tilde{\Sigma}_j}, \quad \text{odd} \quad j < \frac{N}{2}, \tag{46a}$$

$$a_c^{(N)} = \ln\left[\frac{(\xi_j + \sqrt{\xi_j^2 - \tilde{\Sigma}_j^2})(\xi_{j+1} + \sqrt{\xi_{j+1}^2 - \tilde{\Sigma}_j^2})}{\tilde{\Sigma}_j^2} \right] \quad \text{even} \quad j < \frac{N}{2}, \tag{46b}$$

$$\beta a_c^{(N)} = \ln(\xi_0^{-1} + \sqrt{\xi_0^{-2} - 1}). \tag{46c}$$

Even N, $\beta < 1/2$, $\mu_c = \pi$. Using Eq. (39) with $\mu_c = \pi$ and following the same procedure, we arrive to the following system of transcendental equations which define a_c:

$$\beta a_c^{(N)} = \frac{\pi}{2} - \arcsin\left(\frac{1}{\xi_0}\right), \tag{47a}$$

$$a_c^{(N)} = \pi - \arcsin\frac{\xi_{j+1}}{\tilde{\Sigma}_j} - \arcsin\frac{\xi_j}{\tilde{\Sigma}_j} \quad \text{for even} \quad j < N/2, \tag{47b}$$

$$a_c^{(N)} = \ln\left[\frac{(\xi_j + \sqrt{\xi_j^2 - \tilde{\Sigma}_j^2})(\xi_{j+1} + \sqrt{\xi_{j+1}^2 - \tilde{\Sigma}_j^2})}{\tilde{\Sigma}_j^2} \right] \quad \text{for odd} \quad j < N/2. \tag{47c}$$

Now we consider infinitely long JJ. Similar to the finite LJJ, a_c is not zero only for even *N*. For calculation of the

TABLE II. The values of $a_c^{(N)}$ for $\beta=1$ (accuracy of calculation is ± 0.0001).

N	a_c^N	Solution of Eq. (46)
2	1.4639	$\xi_0=0.4392$
4	1.1772	$\xi_0=0.5628$, $\xi_2=1.1469$
6	1.0060	$\xi_0=0.6451$, $\xi_2=1.1807$, $\xi_3=1.3141$

crossover distance in this case we use Eqs. (46), with limit $\beta\to\infty$ and $\mu_0=0$. This modifies Eq. (46a) for $j=1$,

$$a_c^{(N)}=\frac{3}{4}\pi-\arcsin\frac{\xi_2}{\sqrt{2}}. \tag{48}$$

The rest of equations from the system (46) remain the same.

To give an example, the values of $a_c^{(N)}$ calculated for $\beta=1$, $\beta=1/4$, and $\beta=\infty$ are presented in Table II, Table III, and Table IV, respectively, and are in accordance with Table I. This technique of solving numerically a system of transcendental equations is rather effective and can be used to obtain the plots $a_c^{(N)}(\beta)$ shown in Fig. 4. Note that these plots exactly coincide with the ones obtained in Sec. III A using stability analysis for flat phase state.

The coincidence of the crossover distances obtained in two different ways implies that the transition between AFM state and flat phase state at $a=a_c$ happens because AFM solution just cease to exist. It was believed before[19] that transition takes place because one of the states has lower energy. Now it is also clear why in Ref. 19 the hysteresis around a_c was never seen. Hysteresis usually takes place when one has two stable solutions having different energies.

We can draw possible states of the system as a pitchfork bifurcation diagram shown schematically in Fig. 6. At small $a<a_c$ the flat state is the only solution and it is stable. At $a=a_c$ the flat phase solution looses its stability, and it is unstable at $a>a_c$ as indicated by the dotted line. At the same time, at $a=a_c$ two new solutions appear. Both correspond to AFM ordered chain of semifluxons but with different sign.

IV. CONCLUSIONS

We have studied analytically the ground states in a 0-π-LJJ with different number of facets of the length $a\sim\lambda_J$. We have shown that in the general case there is a crossover distance $a_c^{(N)}$ such that if the facet length $a<a_c^{(N)}$, the system is in the flat phase state ($\mu=$const) and contains no magnetic flux. In contrast, if $a>a_c^{(N)}$, the ground state consists of fractional vortices, each pinned at the phase discontinuity point. There may be more than one such state, especially for large N, but we focus our attention on the most natural one—AFM ordered chain of semifluxons. The system chooses between flat phase state and AFM ordered chain of semifluxons not because of the energy competition as it was suggested earlier,[19] but because there is only one stable solution for given a, as shown in the bifurcation diagram Fig. 6: for $a<a_c^{(N)}$ AFM ordered semifluxon solution does not exist, while a flat phase state exists and is stable; for $a>a_c^{(N)}$ flat phase solution $\mu=$const exists but is unstable, so the state is AFM ordered semifluxon chain. We have calculated the crossover distances $a_c^{(N)}$ and summarize our results as follows.

(a) For odd N, $a_c=0$, semifluxons are always present.

(b) For even N $a_c\geqslant 0$. The dependences of $a_c^{(2)}$, $a_c^{(4)}$, and $a_c^{(6)}$ on b are shown in Fig. 4. In particular, for $b=a/2$, $a_c^{(N)}=0$ and semifluxons are always present, for all other b, $a_c>0$.

Our calculations of a_c agree with previous numerical and analytical results,[11,19,20] but cover also the cases of larger N, arbitrary edge facets length b and have much higher accuracy. We also show that in many cases the size of the edge facets b can drastically affect the state of the whole system, especially when $b\approx a/2$ or $b\to 0$ and $N=2$, as can be seen from Fig. 4.

We stress that we derived the position of bifurcation point a_c approaching it from both flat phase state (from the left in

TABLE III. The values of $a_c^{(N)}$ for $\beta=1/4$ (accuracy of calculation is ± 0.0001).

N	a_c^N	Solution of Eq. (47)
2	2.9277	$\xi_0=1.34429$
4	1.2546	$\xi_0=1.0513$, $\xi_2=1.3734$
6	0.9833	$\xi_0=1.0310$, $\xi_2=1.2352$, $\xi_3=1.3233$

TABLE IV. The values of $a_c^{(N)}$ for $\beta=\infty$ (accuracy of calculation is ± 0.0001).

N	a_c^N	Solution of Eqs. (46) and (48)
2	$\pi/2$	
4	1.3063	$\xi_2=1.2266$
6	1.1343	$\xi_2=1.3290$, $\xi_3=1.6058$
8	1.0146	$\xi_2=1.3772$, $\xi_3=1.7641$, $\xi_4=1.9065$

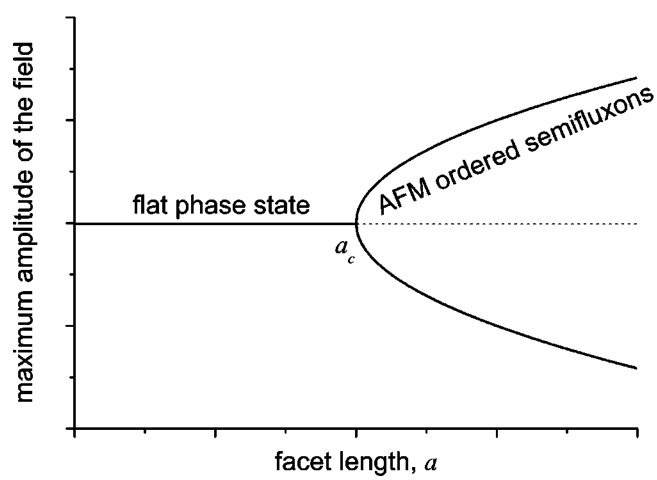

FIG. 6. The sketch of the bifurcation diagram which shows the transition from flat phase state to the state with AFM ordered semifluxon chain.

Fig. 6) and from the state with AFM ordered chain of semifluxons (from the right in Fig. 6), and we got the same results. In the first approach, the system of equations [Eqs. (29) for $b>a/2$ or Eqs. (31) for $b<a/2$], that describe the (in)stability of the flat phase state, is particularly easy to solve numerically and the reader is encouraged to do so for his/her favorite values of N and b just setting proper seed value for a_c. Nevertheless, our derivation of more complex equations (46) for $b>a/2$ and Eqs. (47) for $b<a/2$, which describes the disappearance of AFM ordered semifluxon chain and gives the same values of a_c, is not useless. This approach, although more complex, allows us to find the existence region for more complex semifluxon states such as $\uparrow\uparrow\downarrow\downarrow$, which will be discussed elsewhere using the results obtained here.

We have also found that the crossover distance $a_c \propto 1/\sqrt{N}$ for large N, see Eqs. (35) and (36) or Eqs. (C9) and (C10) of Appendix C. Having a fixed, the longer 0-π-LJJ (larger N) favors configurations with semifluxons and, therefore, with magnetic flux, while shorter LJJ (smaller N) favors the state without flux. Instead, if we fix the total LJJ length, the LJJ with smaller a (large N) will favor flat phase state, while the LJJ with larger a (small N) will favor the state with semifluxons.

In the future, it is quite interesting to consider the possibility to have less natural states such as $\uparrow\uparrow\downarrow\downarrow$. This will correspond to the additional branches on the bifurcation diagram and there will be clearly a minimum distance $a_c(\uparrow\uparrow\downarrow\downarrow)>a_c(\uparrow\downarrow\uparrow\downarrow)$ [$a_c(\uparrow\downarrow\uparrow\downarrow)$ is the one found here] for which such a state is stable. For $a>a_c(\uparrow\uparrow\downarrow\downarrow)$ there will be energy competition between various states, e.g., between $\uparrow\downarrow\uparrow\downarrow$ and $\uparrow\uparrow\downarrow\downarrow$. Next, in terms of studying classical and quantum tunneling between various states such as $\uparrow\uparrow\downarrow\downarrow$ and $\uparrow\downarrow\uparrow\downarrow$, it is interesting to consider how a_c depends on the applied magnetic field and bias current.

ACKNOWLEDGMENTS

This work was supported by the Deutsche Forschungsgemeinschaft (DFG) within Project No. Si 704/2-1, partially supported by the ESF programs "Vortex," "Pi-shift," and RFBR Grants Nos. 03-01-06122 and 1716.2003.1.

APPENDIX A: THE ONLY "OTHER" VALUE OF $\mu_c=\pi/2$

Now we show that if $a_c=0$, then $\mu_c=\pi/2$. Let us subtract expression (9) for two end values of μ in the nth odd interval: $\mu=\mu_n$ and $\mu=\mu_{n+1}$. For them $x_{n+1}-x_n\approx\sqrt{\epsilon}$, $\alpha_n\approx\pm\sqrt{2}$, x_{2n}^* are defined by Eq. (8). Having this, we receive

$$\begin{aligned}\epsilon(\tilde{\mu}_{n+1}-\tilde{\mu}_n)&=2\,\mathrm{am}[(x_{n+1}-x_n^*)/\alpha_n,m_n]\\&\quad-2\,\mathrm{am}[(x_n-x_n^*)/\alpha_n,m_n]\\&\approx\frac{2\sqrt{\epsilon}}{\alpha_n}\mathrm{dn}\left(\frac{x_n-x_n^*}{\alpha_n},\alpha_n^2\right)+O(\epsilon),\end{aligned}$$

where $\mathrm{dn}(x,m)=\sqrt{1-m\sin^2\mathrm{am}(x,m)}$ is the Jacobi elliptic function. There is only one term of the order of $\sqrt{\epsilon}$ in this expression. Thus this term equals zero. Using expression (8) for x_n^* $[x_n^*=x_n-\alpha_nF(\mu_n/2,m_n)]$ with substitution $m_n\approx 2$ and we get $\mathrm{dn}[F(\mu_c/2,2),2]=0$, which has the only solution inside the interval $0<\mu<\pi$: $\mu_c=\pi/2$.

APPENDIX B: BEHAVIOR OF THE FUNCTION $\beta_1(a_c)$

Let us consider Eqs. (29) for odd $N/2$. Even $N/2$ can be considered similarly. We show that $\beta_1(a_c)$ is a decreasing convex function within the interval from $a_c=0$ to the first discontinuity.

Let us derive the system of equations for β_j with odd j. Due to the specific domains for $\tan(x)$ and $\mathrm{arctanh}(x)$ one concludes from Eqs. (29) that for odd j,

$$0\leqslant a_c<\frac{\pi}{2}, \tag{B1a}$$

$$-\frac{\pi}{4}<\beta_j<\frac{\pi}{4}, \tag{B1b}$$

$$-\frac{\pi}{4}<a_c+\beta_j<\frac{\pi}{4}. \tag{B1c}$$

We eliminate β_j with even j from Eq. (29b) using Eq. (29c).

$$\beta_{2n+1}=-a_c+\arctan[\tanh(a_c+\mathrm{arctanh}\tan\beta_{2n+3})], \tag{B2}$$

$$\beta_{N/2}=-\frac{a_c}{2}. \tag{B3}$$

Hereafter in this section $n=0,1,\ldots,(N-6)/4$, unless otherwise specified.

Using these equations and induction method we prove the following inequalities:

$$\beta_{2n-1}\leqslant\beta_{2n+1}, \tag{B4}$$

$$\beta'_{2n+1}<0, \tag{B5}$$

$$\beta''_{2n+1}<0. \tag{B6}$$

Proofs. Let us start with inequality (B4). We find directly from the plots that $\beta_{N/2-4}\leqslant\beta_{N/2-2}\leqslant\beta_{N/2}$. Assume that $\beta_{2k+1}\leqslant\beta_{2k+3}$ for arbitrary k and consider the expression $\tan(\beta_{2n-1}-\beta_{2n+1})$. Using Eq. (B2) we get $\mathrm{sgn}[\tan(\beta_{2k-1}-\beta_{2k+1})]=\mathrm{sgn}[\sin(\beta_{2k+1}-\beta_{2k+3})]\leqslant 0$, i.e.,

$$\beta_{2k-1}\leqslant\beta_{2k+1} \tag{B7}$$

for all possible k.

To prove the inequality (B5) let us differentiate Eq. (B2) with respect to a_c,

$$\beta'_{2n+1}=\frac{\beta'_{2n+3}-2\cos(2\beta_{2n+3})\sinh^2 Z}{\cos(2\beta_{2n+3})\cosh(2Z)}, \tag{B8}$$

where $Z=a_c+\text{arctanh}\tan(\beta_{2n+3})$. Using Eqs. (B3) and (B8) we see from the graph of $\beta'_{N/2-2}$ that $\beta'_{N/2-2}\leqslant 0$. Suppose that $\beta'_{2k+3}\leqslant 0$ for arbitrary $k>0$. Then we have from Eq. (B8) due to the restrictions (B1) that $\beta'_{2k+1}<0$ for all k. The second statement is proven. We need the following three simple consequences from this inequality.

(1) Since $\beta_{2k+1}(0)=0$ (which can be checked directly), we obtain that $\beta_{2k+1}(a_c)\leqslant 0$ for all k. Thus Eq. (B1) becomes

$$0\leqslant a_c<\frac{\pi}{2},\quad -\frac{\pi}{4}<\beta_{2n+1}\leqslant 0. \tag{B9}$$

(2) Similarly to the proof of Eq. (B7) we can prove that

$$\beta'_{2n-1}\leqslant\beta'_{2n+1}. \tag{B10}$$

(3) Using Eqs. (B3) and (B10) one obtains the restriction for derivatives:

$$\beta'_{2n+1}\leqslant -\frac{1}{2}. \tag{B11}$$

To represent the simplest proof of the last inequality (B6) we rewrite Eq. (B2) in symbolic form

$$f(a_c+\beta_{2n+1})-a_c=f(\beta_{2n+3}), \tag{B12}$$

where $f(x)=\text{arctanh}[\tan(x)]$. We differentiate this equation twice with respect to a_c and solve for β''_{2n+1},

$$\beta''_{2n+1}=\frac{-f''(a_c+\beta_{2n+1})(\beta'_{2n+1}+1)^2+f''(\beta_{2n+3})(\beta'_{2n+3})^2+f'(\beta_{2n+3})\beta''_{2n+3}}{f'(a_c+\beta_{2n+1})}, \tag{B13}$$

where prime means derivative with respect to argument of the function [remember that $\beta_j=\beta_j(a_c)$]. Now the statement can be proven by induction using the facts that $\beta''_{N/2}=0$, $f(-x)=-f(x)$, $f'(x)>0$, $\text{sgn}[f''(x)]=\text{sgn}(x)$.

If $a_c+\beta_{2n+1}\geqslant 0$, all terms in the numerator of Eq. (B13) are nonpositive and we immediately conclude that (B6) is true.

If $a_c+\beta_{2n+1}<0$, the first term is positive and one should demonstrate that the whole expression on the right-hand side (rhs) of Eq. (B13) stays nonpositive anyway. For this we show that the sum of the first and second terms is nonpositive. First, since

$$\beta_{2n+3}<\beta_{2n+1}<\beta_{2n+1}+a_c<0,$$

we can write that

$$|\beta_{2n+3}|>|\beta_{2n+1}+a_c|. \tag{B14}$$

Second, since $\beta'_{2n+3}<\beta'_{2n+1}$ (B10) and $\beta_{2n+1}<-\frac{1}{2}$ (B11) we have

$$|\beta'_{2n+3}|>|\beta'_{2n+1}+1|. \tag{B15}$$

Taking into account (B14) and that $f'''(x)>0$, we have

$$f''(a_c+\beta_{2n+1})\leqslant f''(\beta_{2n+3}). \tag{B16}$$

Consequently from Eqs. (B15) and (B16) we see that the absolute value of the second term in the numerator of Eq. (B13) is larger in comparison with the absolute value of the first term, which leads to the nonpositive rhs of Eq. (B13).

APPENDIX C: BEHAVIOR OF INSTABILITY POINT AT LARGE *N*; ASYMPTOTIC RELATION FOR ARBITRARY β

The analysis in this section is based on the fact that $(\beta_{j+2}-\beta_j)/\beta_j\ll 1$ for $N\to\infty$. This allows us to approximate the function β_j of discrete parameter j by the pair of continuous functions and derive the first-order ordinary differential equation with boundary conditions for one of them. Solving it one gets the implicit relation between a_c and N. Without loss of generality we assume that $N/4$ is odd in this section.

First, we consider the case $\beta>1/2$. Let us introduce two functions, corresponding to odd and even intervals: $A(n)=\beta_{2n-1}$, $B(n)=\beta_{2n}$, $n=1,2,\ldots,N/4$ and rewrite the system (29) in the following form:

$$A(1)=-\arctan[\tanh(\beta a_c)], \tag{C1}$$

$$\tan[a_c+A(n)]=-\tanh[B(n)], \tag{C2}$$

$$\tanh[a_c+B(n)]=-\tan[A(n+1)], \tag{C3}$$

$$A(N/4-2)\approx A(N/4)=-\frac{a_c}{2}. \tag{C4}$$

The index $n=1,2\ldots,N/4-2$ in Eq. (C2) and $n=1,2\ldots,N/4-1$ in Eq. (C3).

Now we may write $A(n+1)\approx A(n)+A'(n)$, $A'(n)\ll A(n)$, where by definition

$$A'(n)=\lim_{\Delta n\to 0}\frac{A(n+\Delta n)-A(n)}{\Delta n}.$$

Express $B(n)$ in terms of $A(n)$ using Eq. (C2) and expand the rhs of Eq. (C3) in series with respect to A' keeping only linear term in A'. Then we have (we now write "=" instead of "≈")

$$A'=f(A)=\frac{\cos A[\sin a_c-\cos(a_c+2A)\tanh a_c]}{\cos(a_c+A)-\sin(a_c+A)\tanh a_c}, \tag{C5}$$

$$A(1)=-\arctan[\tanh(\beta a_c)],\quad A(N/4)=-a_c/2, \tag{C6}$$

where A' is positive, since $A(n+1)>A(n)$. The latter is consequence of Eqs. (C2), (C3), and the property of the increasing convex function f: $f(x_1+x_2)<f(x_1)+f(x_2)$. Thus the above equation may be formally integrated

$$\int_{A(1)}^{-a_c/2} \frac{d\beta}{f(\beta)} = \left(\frac{N}{4}-3\right). \tag{C7}$$

Although integration can be done explicitly, we stay with this symbolic form for the sake of simplicity.

Similarly, for $\beta<1/2$ we get the same Eq. (C7) with different function f and boundary condition $A(1) = -\text{arctanh}[\tan(\beta a_c)]$:

$$f(A) = \frac{\cosh A[\sinh a_c - \cosh(a_c+2A)\tan a_c]}{\cosh(a_c+A)+\sinh(a_c+A)\tan a_c}. \tag{C8}$$

with negative A'.

Equation (C7) gives us essentially function $N(a_c)$ rather then desirable $a_c(N)$. Fortunately $N(a_c)$ may be simply inverted since $a_c \ll 1$ everywhere in these calculations. In fact, one can expand left-handside of Eq. (C7) in powers of a_c, keeping only the leading term, which is of the order of a_c^{-2}. Thus

$$a_c \approx 2\sqrt{\frac{g(\beta)}{N}}, \tag{C9}$$

where

$$g(\beta) = \sqrt{3}\ \arctan[\sqrt{3}(2\beta-1)], \quad \beta>\frac{1}{2}, \tag{C10a}$$

$$g(\beta) = \sqrt{3}\ \arctan[\sqrt{3}(1-2\beta)], \quad \beta<\frac{1}{2}. \tag{C10b}$$

In particular, for $\beta\to\infty$ we have $g=\pi\sqrt{3}/2$ (see Fig. 7).

Thus for large N and any length $b=\beta a$ of the end facets we have derived asymptotic relation $a_c \sim N^{-1/2}$, which is in agreement with equations of Sec. III A 1.

Now we derive applicability condition for the equations of this section. Equation (C7) can be used for N such that

$$\left|\frac{\max A'}{A}\right| \ll 1. \tag{C11}$$

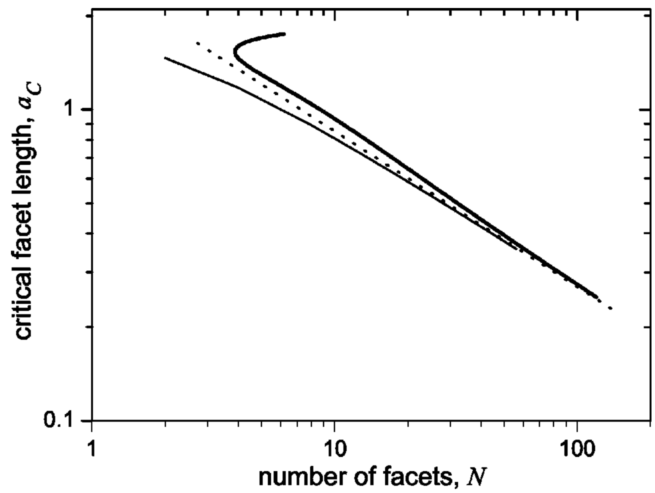

FIG. 7. Asymptotic behavior of $a_c(N)$ for $\beta=1$. Solid bold line is received using Eq. (C7); dotted line corresponds to Eq. (C9); solid thin line is result of numerical solution of the system (29).

Investigation of the series in a_c of the ratio $(\max A')/A$ shows that it does not have local extremum. Thus its maximum value can be taken only at the end points of the integration interval: $A=-a_c/2$ or $A=A(1)$. One can show that this point is $A(1)$ for all finite values of β as well as for infinite β.

Using leading (linear) term of the series of A' in a_c we get from Eqs. (C5) and (C8):

$$A' \approx +2a_c \sin^2(A), \quad \beta>1/2, \tag{C12}$$

$$A' \approx -2a_c \sinh^2(A), \quad \beta<1/2. \tag{C13}$$

Together with relation (C9) and the fact that $A(1) \approx -\beta a_c$ for $\beta a_c \ll 1$, $-\pi/4 \lesssim A(1) < 0$ for $\beta a_c \gtrsim 1$ and $A(1) = -\pi/4$ for $\beta\to\infty$, we arrive to

$$N \gg 8g, \quad \beta a_c \ll 1, \tag{C14}$$

$$N \gg 2\sqrt{2}g, \quad \beta\to\infty \quad \text{or} \quad \beta a_c \gtrsim 1. \tag{C15}$$

*Electronic address: zenchuk@itp.ac.ru
†Electronic address: gold@uni-tuebingen.de URL: http://www.geocities.com/e_goldobin

[1] C.C. Tsuei and J.R. Kirtley, Rev. Mod. Phys. **72**, 969 (2000).
[2] H.J.H. Smilde, Ariando, D.H.A. Blank, G.J. Gerritsma, H. Hilgenkamp, and H. Rogalla, Phys. Rev. Lett. **88**, 057004 (2002).
[3] V.V. Ryazanov, V.A. Oboznov, A.Y. Rusanov, A.V. Veretennikov, A.A. Golubov, and J. Aarts, Phys. Rev. Lett. **86**, 2427 (2001).
[4] V.V. Ryazanov, V.A. Oboznov, A.V. Veretennikov, and A.Y. Rusanov, Phys. Rev. B **65**, 020501 (2001).
[5] T. Kontos, M. Aprili, J. Lesueur, F. Genêt, B. Stephanidis, and R. Boursier, Phys. Rev. Lett. **89**, 137007 (2002).
[6] E. Goldobin (unpublished).
[7] G.J. Gerritsma, First International Workshop on the Symmetry in Macroscopic Quantum States, Augsburg, Germany, 2002 (unpublished). See http://www.Physik.Uni-Augsburg.DE/exp6/pishift/
[8] E. Terzioglu and M.R. Beasley, IEEE Trans. Appl. Supercond. **8**, 48 (1998).
[9] L.B. Ioffe, V.B. Geshkenbein, M.V. Feigel'man, A.L. Faucheère, and G. Blatter, Nature (London) **398**, 679 (1999).
[10] R.G. Mints, I. Papiashvili, J.R. Kirtley, H. Hilgenkamp, G. Hammerl, and J. Mannhart, Phys. Rev. Lett. **89**, 067004 (2002).
[11] T. Kato and M. Imada, J. Phys. Soc. Jpn. **66**, 1445 (1997).
[12] N. Stefanakis, Phys. Rev. B **66**, 214524 (2002).
[13] J.H. Xu, J.H. Miller, and C.S. Ting, Phys. Rev. B **51**, 11 958 (1995).

[14] E. Goldobin, D. Koelle, and R. Kleiner, Phys. Rev. B **66**, 100508 (2002).
[15] H. Hilgenkamp, Ariando, H.-J.H. Smilde, D.H.A. Blank, G. Rijnders, H. Rogalla, J.R. Kirtley, and C.C. Tsuei, Nature (London) **422**, 50 (2003).
[16] J.R. Kirtley, C.C. Tsuei, M. Rupp, J.Z. Sun, L.S. Yu-Jahnes, A. Gupta, M.B. Ketchen, K.A. Moler, and M. Bhushan, Phys. Rev. Lett. **76**, 1336 (1996).
[17] J.R. Kirtley, C.C. Tsuei, and K.A. Moler, Science **285**, 1373 (1999).
[18] A. Sugimoto, T. Yamaguchi, and I. Iguchi, Physica C **367**, 28 (2002).
[19] E. Goldobin, D. Koelle, and R. Kleiner, Phys. Rev. B **67**, 224515 (2003); cond-mat/0209214 (unpublished).
[20] A.B. Kuklov, V.S. Boyko, and J. Malinsky, Phys. Rev. B **51**, 11 965 (1995), **55**, 11 878(E) (1997).